ASTM INTERNATIONAL

Journal of
Testing and Evaluation

M. Naghibi,[1] H. Abuel-Naga,[2] and R. Orense[3]

DOI: 10.1520/JTE20160002

Modified Odometer Cell to Measure Electrical Resistivity of Clays Undergoing Consolidation Process

VOL. 45 / NO. 4 / JULY 2017

Journal of Testing and Evaluation

doi:10.1520/JTE20160002 / Vol. 45 / No. 4 / July 2017 / available online at www.astm.org

M. Naghibi,[1] H. Abuel-Naga,[2] and R. Orense[3]

Modified Odometer Cell to Measure Electrical Resistivity of Clays Undergoing Consolidation Process

Reference

Naghibi, M., Abuel-Naga, H., and Orense, R., "Modified Odometer Cell to Measure Electrical Resistivity of Clays Undergoing Consolidation Process," *Journal of Testing and Evaluation*, Vol. 45, No. 4, 2017, pp. 1261–1269, http://dx.doi.org/10.1520/JTE20160002. ISSN 0090-3973

ABSTRACT

Electrical resistivity is used widely to evaluate various soil behavior and properties. Furthermore, it controls the power consumption during the electro-osmosis consolidation process. This paper discusses the modifications made on the conventional odometer test apparatus to measure the electrical resistivity of a clay specimen undergoing consolidation at different vertical effective stress levels using the four-electrode Wenner array method. Extensive numerical calibrations were also conducted to investigate the effect of boundary conditions of the test set up on the electrical resistivity values and, based on the results obtained, a general calibration equation is introduced. The validity of the proposed calibration equation is confirmed experimentally using different materials with known electrical resistivity values. Finally, three different sets of electrical resistivity results during the consolidation process are presented and discussed from the modified odometer cell.

Keywords

electrical resistivity, numerical model, laboratory testing, Wenner array

Manuscript received January 1, 2016; accepted for publication May 10, 2016; published online July 29, 2016.

[1] Dept. of Civil and Environmental Engineering, Univ. of Auckland, Auckland 1142, New Zealand (Corresponding author), e-mail: mnag216@aucklanduni.ac.nz

[2] La Trobe Univ., Plenty Rd. and Kingsbury Dr., Melbourne, VIC, Australia

[3] Dept. of Civil and Environmental Engineering, Univ. of Auckland, Auckland 1142, New Zealand

Introduction

Electrical resistivity is a fundamental property of soils. It is a function mainly of moisture content and several other parameters, such as mineralogy, soil structure, texture, temperature, and salt content of the pore water [1–8]. Therefore, several studies have attempted to determine, indirectly, the soil's physical properties using its electrical resistivity value [9–14].

Electro-osmosis (EO) consolidation is one of the ground-improvement techniques that could strengthen soft soils by subjecting it to dc electric potential gradients. Under the influence of an

electric potential, the cations in the body of a saturated soil mass are drawn to the cathode and the anions to the anode. Ions carry their water of hydration and exert a viscous drag on the water around them. This type of soil behavior subjected to dc electric potential gradient establishes a net water flow toward the cathode and creates negative pore water pressure that produces soil consolidation [15–20].

The electrical properties of saturated soft clays, such as electrical resistivity/conductivity, control the efficiency of EO consolidation method as it has a direct effect on the power consumption. Mitchell and Soga [20] state that the EO power consumption per unit volume of flow can be expressed as:

$$\frac{P}{q_h} = \frac{\Delta E}{\rho k_e} \tag{1}$$

where:

P = the power consumption,
q_h = the flow rate,
ΔE = the applied electrical potential,
ρ = the electrical resistivity of soil, and
k_e = coefficient of electro-osmotic hydraulic conductivity.

According to Casagrande [21] and Mitchell and Soga [20], k_e is almost similar for all types of soils. Therefore, the EO power consumption per unit volume of flow under a specified ΔE is a function of mainly the soil's electrical resistivity. As the electrical resistivity is a function of void ratio of the consolidated soils, the evolution of the soil's electrical resistivity during the consolidation process, which involves decreasing void ratio, should be considered in the EO consolidation design process to assess the required change in power consumption with time. Modified odometer cells that employ Wenner the four-electrode method [22–24] to determine the evolution of soil electrical resistivity as the effective stress (or void ratio) changes were proposed by several researchers [2,10,11,25–27].

The Wenner four-electrode method is used usually to measure soil resistivity in the field. The method involves using four copper electrodes placed in equal separation, a (cm), in a straight line on the surface. A voltage is applied between the outer electrodes where the corresponding current, I, and the voltage drop between the inner electrodes, V, are measured. The ac or dc source of current can be used in electrical resistivity measurements [23]. In addition, the electrical resistivity of soil can be studied based on response of soil to the electromagnetic field in specific range of frequencies. In such case, any external electromagnetic interferences should be blocked out [28].

The electrical resistivity, ρ (Ω-m), is then determined as:

$$\rho = 2\pi a\left(\frac{V}{I}\right) \tag{2}$$

It should be mentioned that the measured ρ by the Wenner four-electrode method represents the average resistivity of a hemisphere of soil of a radius approximately proportional, in homogenous medium, to the electrode separation, where the term ($2\pi a$) is a geometrical factor defined based on a semi-infinite boundary condition (half-space).

Some researchers used eight equally spaced electrodes inserted through the sides of the cell where four probes are used to make individual resistance measurements as shown in **Fig. 1a** [2,11,25,26]. This probe configuration allows eight resistance measurements where each set of four adjacent probes can be used to produce a resistance measurement. Consequently, the eight measurements well represent the whole test specimen from which an average value can be assigned for the test specimen. However, it should be mentioned that the boundary conditions of this cell do not comply with the boundary conditions of the Wenner method because the cell does not provide the semi-infinite boundary condition required. Furthermore, the thickness of the testing specimen (height of the cell) would not satisfy the hemisphere geometry requirement of the current flow.

FIG. 1 Previous electrical resistivity odometer cells in the literature. [Note: PERP (plane-type electrical resistivity probe) consists of four electrodes installed based on Wenner array configuration.]

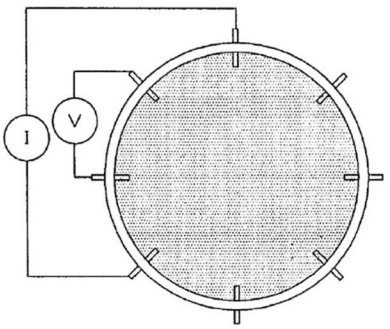

a) Kalinski and Kelly [11, 26]

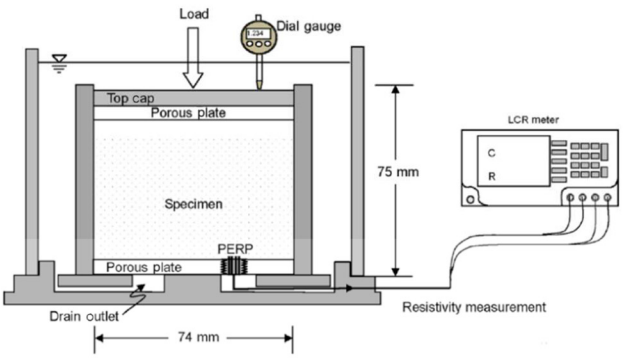

b) Kim et al. [10] and Choo et al. [27]

Kim et al. [10] and Choo et al. [27] attached an electrical resistivity probe into the bottom porous stone of a specially designed odometer, as shown in **Fig. 1b**. As the electrical resistivity probe is small in size compared to the test specimen, the measured resistance value represents only a minimal fraction of the test specimen; therefore, it is not recommended for testing heterogeneous soils. Furthermore, the effect of having bottom porous stone on the resistivity measurement should be assessed, as this boundary should be an electrical insulator in the Wenner method.

In this paper, a simple modification of the conventional odometer apparatus is proposed to measure the evolution of electrical resistivity of saturated soils as the effective stress changes. To align with ASTM D6431-99 [24], dc source of current has been used to measure the electrical resistivity of the soil. Furthermore, a robust calibration protocol for the possible effects of boundary conditions on the electrical resistivity measurements is introduced and validated.

Proposed Modified Electrical Resistivity Odometer Cell

Fig. 2 shows the proposed modification to the conventional odometer cell adopted where the specimen ring is made of polyvinyl chloride (PVC) and can accommodate a 76-mm diameter soil specimen with initial height of 20 mm. Four brass electrodes, equally spaced at 20 mm apart, are embedded into the PVC top cap to measure the electrical resistivity using the Wenner method. To allow for drainage during the consolidation process, a porous stone that rests on a PVC plate is used as the bottom boundary of the testing specimen. However, the geometric boundary conditions of the cell shown in **Fig. 2** do not satisfy the assumptions of Eq 2; therefore, a modified equation is required to reflect the effect of the proposed cell boundary conditions. Rasor and Tinker electrical resistivity meter model SR-2 was used in the tests. It is capable of measuring soil electrical resistivity ranging from 0.1 Ω-m to 3.3 MΩ-m.

Calibration of the Proposed Cell and Results

BACKGROUND

The boundary conditions of the proposed cell that could affect the validity of Eq 2 can be described using the following three dimensionless parameters: S/D, L/S, and α, where L, S, and D are the thickness of the soil specimen, spacing between the electrodes, and radial spacing between the outer electrode and the outer boundary of the tested specimen, respectively, as shown in **Fig. 2**. The term α is expressed as:

$$\alpha = \frac{\mathrm{Th}_{\mathrm{ps}}\rho_{\mathrm{ps}}}{\mathrm{Th}_T\rho_{\mathrm{exp}}} \tag{3}$$

where:

$\mathrm{Th}_{\mathrm{ps}}$ = thickness of porous stone,

Th_T = total thickness of porous stone and the testing specimen,

ρ_{exp} = experimental electrical resistivity of soil specimen, and

ρ_{ps} = electrical resistivity of porous stone.

Therefore, the first two parameters (S/D and L/S) describe the geometric conditions and the last parameter, and α expresses the effect of the electrical resistivity and thickness of

FIG. 2 Proposed modified odometer cell for measuring electrical resistivity.

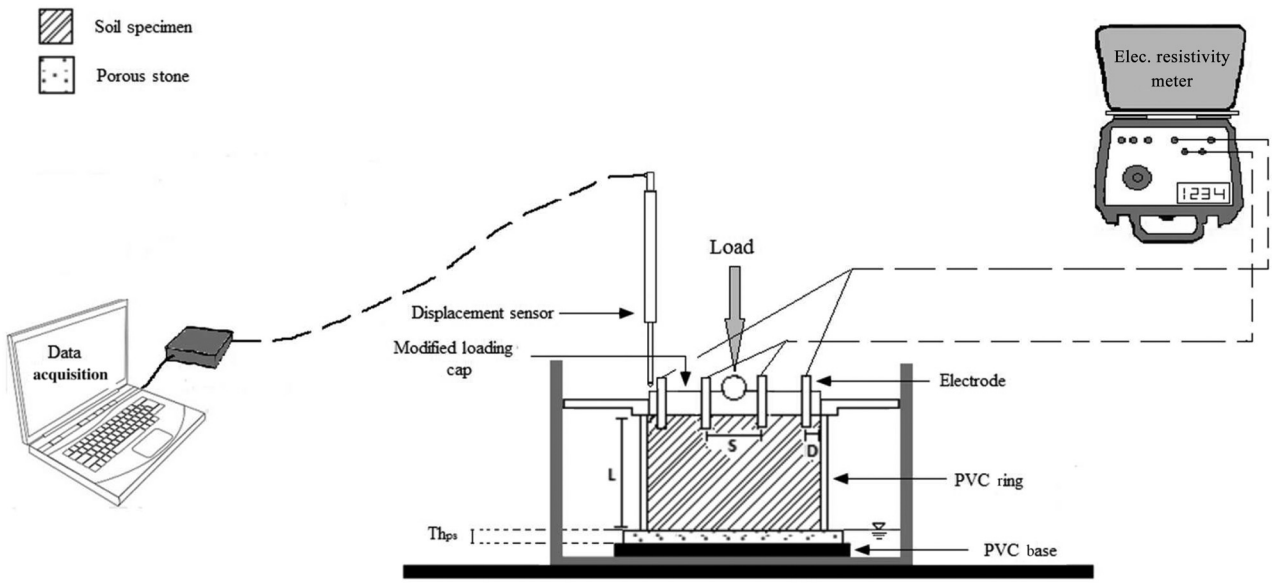

the bottom boundary (porous stone). The deviation of the measured electrical resistivity, ρ_{exp}, using the proposed cell and Eq 2 from the actual electrical resistivity, ρ_{act}, can be expressed as:

$$\beta = \frac{\rho_{act}}{\rho_{exp}} \tag{4}$$

where:

β = the boundary condition calibration factor, that is controlled by the proposed three dimensionless parameters (S/D, L/S, and α).

Therefore, Eq 2 can be modified to determine the actual resistivity (electrical resistivity) using the proposed cell as:

$$\rho_{act} = 2\pi\beta a\frac{V}{I} \tag{5}$$

It should be mentioned that when $L/S = \infty$, it follows that $D/S = \infty$, $\alpha = 0$ (Wenner method condition), and $\beta = 1.0$. A calibration process is conducted in this study to determine the evolution of β as the three dimensionless boundary condition parameters (S/D, L/S, and α) deviate from the Wenner method condition.

CALIBRATION METHODOLOGY

In general, the calibration process involves testing samples of known property value using the proposed measuring technique to establish a relationship (calibration equation) between the measured property and the known property value of the tested sample. In other words, the calibration process involves generating an extensive, well-trusted experimental database for the problem under consideration. Then, exploiting this database we can develop a strong mathematical expression between the output of the proposed measuring technique and the known property of the tested samples, using a robust statistical data-processing tool. The success of the developed calibration equation is usually assessed by its accuracy in determining the known value of the tested material from the output of the proposed measurement technique and its ability to consider precisely the effect of boundary conditions' changes.

In this study, generating the calibration database by experimental means is not an easy task (costly and time consuming) because the proposed calibration factor, β, is affected by several parameters (S/D, L/S, and α); thus, a different approach should be considered. In this study, the calibration database is generated by conducting an extensive numerical experimental program as it offers both time and cost saving. Furthermore, it also eludes the following uncertainties that might affect the outcomes of the investigation if a laboratory experimental approach is used: homogeneity of the tested soil specimens and repeatability of the measurements, and level of saturation of the tested soil specimen.

NUMERICAL CALIBRATION PROGRAM

To develop the required calibration database in this study, 72 numerical experiments were conducted using different combinations of the three dimensionless boundary-condition parameters (S/D, L/S, and α) to investigate their effect on the calibration parameter, β. Based on the electrodes' configuration in the top cap, as shown in **Fig. 2**, the geometric boundary-condition parameter D/S was set constant at a value of 0.4. Furthermore, to cover most of the practical cases, the numerical study for the calibration purposes is limited to the conditions, where $0.25 \leq L/S \leq 2$ and $50\ \Omega\text{-m} \leq \rho_{ps} \leq 500{,}000\ \Omega\text{-m}$.

The finite-element solver FlexPDE was used to solve the following governing equation for the three dimensional steady state electricity flows in soils:

$$\Gamma_E = L_E\nabla(-\Phi_E) \tag{6}$$

where:

Γ_E = electrical current,

L_E = conductivity of electrical flow, and

Φ_E = electrical gradient.

The boundary conditions for the conducted numerical simulation can be described as follows:

- Constant electrical potential is applied at the outer electrodes.
- No current flow boundary is located at the top of the specimen, sides of the testing specimen, and the bottom porous stone.

The following assumptions were also adopted in this study:

- No voltage losses between the electrodes and the soil (perfect contact condition).
- Ohm's law is applicable.
- The electrical properties of the considered porous medium are isotropic and homogenous.

NUMERICAL CALIBRATION RESULTS

Fig. 3 shows the effect of α and L/S on calibration factor, β, for $D/S = 0.4$. The results indicated that for different L/S, the calibration factor, β, remains constant for $\alpha > 1$. However, for $\alpha < 1$, the calibration factor, β, increases as α decreases for different L/S values. As $Th_T > Th_{ps}$ and ρ_{exp} is a function of ρ_{act} and ρ_{ps}, the condition of $\alpha > 1$ represents the case where $\rho_{act} < \rho_{ps}$. Thus, $\alpha = 1$ would be a threshold value and beyond that, electrical resistance of the bottom porous stone will have insignificant effect on the current flow configuration; consequently, β remains constant for $\alpha > 1$. On the other hand, in the case of $\alpha < 1$, decreasing the electrical resistance of the bottom porous stone will affect the current flow configuration; consequently, β changes for $\alpha < 1$. Furthermore, the results shown in **Fig. 3** show that at constant α, as L/S increases, β increases. **Fig. 4** shows the evolution of β as L/S increases for $D/S = 0.4$ and $\alpha > 1$. This can be explained in terms of the ratio between

FIG. 3 Relationship between α and calibration factor, β ($D/S = 0.4$).

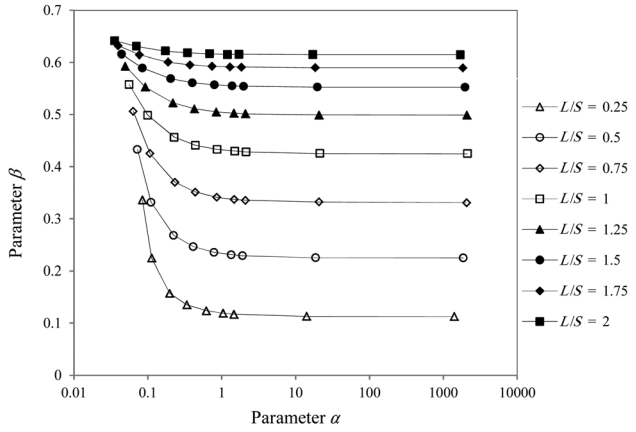

the thickness of the tested specimen, L, and the effective depth of Wenner method, d_e, that can be defined as the depth below which insignificant current is passing through the soil. For the Wenner condition, the ratio $L/d_e = \infty$. Therefore, as L increases, L/d_e increases, and the value of β should move closer to Wenner condition ($\beta = 1$). Thus, β will increase as L/S increases.

Using the results shown in **Fig. 3**, a correlation equation using MATLAB is developed to predict β as follows, where the correlation factor, R^2, is 0.93:

$$\beta = 0.3885 - 0.128\left(\frac{L}{S}\right)^2 + 0.157\alpha\left(\frac{L}{S}\right) - 0.629\alpha + 0.48\left(\frac{L}{S}\right) + 0.202 \quad (7)$$

On the other hand, for $\alpha > 1$, the following equation could be obtained where $R^2 = 0.999$:

FIG. 4 Calibration curve for $\alpha > 1$ ($D/S = 0.4$).

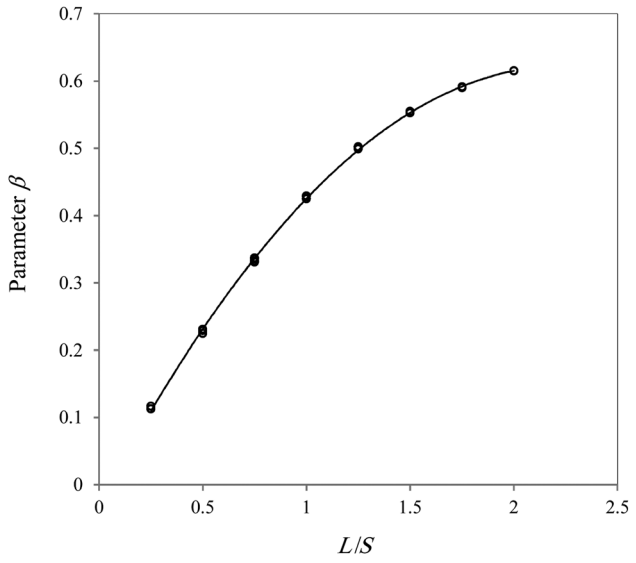

$$\beta = -0.132\left(\frac{L}{S}\right)^2 + 0.586\left(\frac{L}{S}\right) - 0.029 \quad (8)$$

Note that as mentioned above, the above equations are valid for the experimental setup used in the tests, i.e., $D/S = 0.4$. For cell dimensions different from the one employed here, the proposed calibration approach could be extended and used to develop suitable calibration equations. However, it is worthy to mention that subsequent analyses showed that within normal range of D/S (i.e., $0.2 \leq D/S \leq 1.0$), the values of electrical resistivity are not significantly affected by changes in D/S.

Experimental Validation of the Numerical Results

CASE OF $\alpha > 1$

To check the validity of the proposed numerically generated calibration factor for the case where $\alpha > 1$, a special test setup was designed as shown in **Fig. 5**. To allow assessing the effect of changing L/S on β, a liquid of known electrical resistance is used as the testing material. In addition, the data from Rinaldi and Cuestas [29] and ASTM D6431-99 [24] are used for comparison.

The test setup involves the use of PVC inner odometer ring and the modified PVC top cap that includes the Wenner four-electrode arrangement. The top cap is attached to the bottom of the odometer ring as shown in **Fig. 5** and the top boundary of the odometer ring is open to the air (perfect electrical insulator); therefore, $\alpha > 1.0$.

The odometer ring was filled with different types of deaerated water with varying salinity levels (i.e., distilled water,

FIG. 5 Experimental apparatus for calibrating the electrical resistivity in the laboratory ($\alpha > 1.0$).

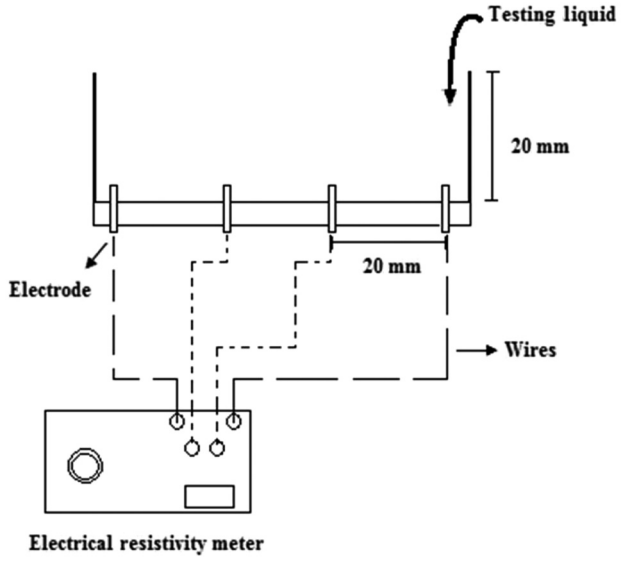

FIG. 6

Evaluation of numerical calibration factors for different testing liquids ($\alpha > 1.0$). (Note: Coordinate in vertical axis is in logarithmic scale.)

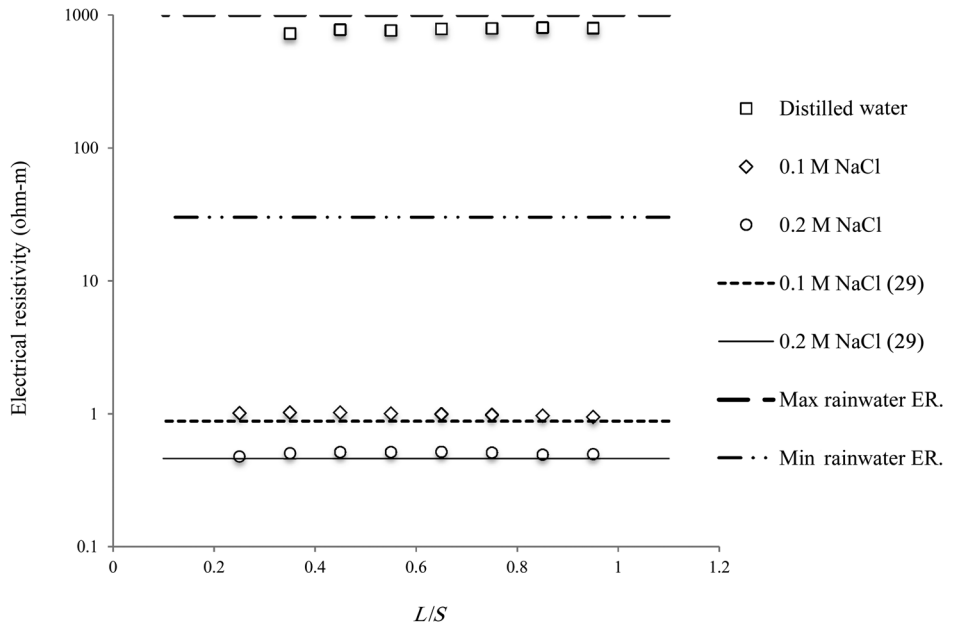

with 0.1 M NaCl, and with 0.2 M NaCl). The height of water in the ring varies between 5 to 19 mm to assess the effect of L/S on β. Tests were conducted at a room temperature of 20°C. **Fig. 6** shows a comparison between ρ_{act}-L/S relationships produced in this study (measured experimentally and calibrated numerically) and previous literature [24,29] for different solutions. As good agreement can be observed, the validity of the numerical calibration method is confirmed for the case of $\alpha > 1.0$.

CASE OF $\alpha \leq 1$

To evaluate the calibration factors for $\alpha \leq 1$, the proposed odometer cell in **Fig. 2** was used. Reconstituted specimens made of New Zealand kaolin clay compacted at different moisture contents were used for the calibration purpose. The tested specimen was installed in the setup shown in **Fig. 2** where different bottom boundary conditions (i.e., PVC, saturated porous stone) are used. The electrical resistivity of the saturated porous stone is determined using the setup shown in **Fig. 5**.

The validation process involves using the PVC bottom boundary condition (electrical insulator) to determine the actual electrical resistivity value of the tested soil specimen. In this case, $\alpha > 1.0$ and the calibration equation is already validated in the previous section. Then, the PVC bottom boundary condition was replaced by the saturated porous stone and the calibrated electrical resistivity under this condition using Eq 6 is compared with the actual electrical resistivity value of the tested soil specimen. As the values of electrical resistivity of the tested specimens are different because the tested specimens have different moisture contents, α for each tested specimen is different. **Fig. 7** shows the measured ρ_{exp} and the corresponding α for each testing specimen. **Fig. 8** shows the results of the validation process where the calibrated electrical resistivity values using PVC and porous stone are compared at different moisture contents and good agreement can be observed.

Application Experiments

With the proposed robust calibration factors, the modified odometer can be trusted to measure the electrical resistivity of soils during the consolidation processes. To illustrate this, several series of consolidation experiments were conducted to

FIG. 7 Relationship between geophysical number (α) and apparent electrical resistivity for pure New Zealand kaolin clay and porous stone.

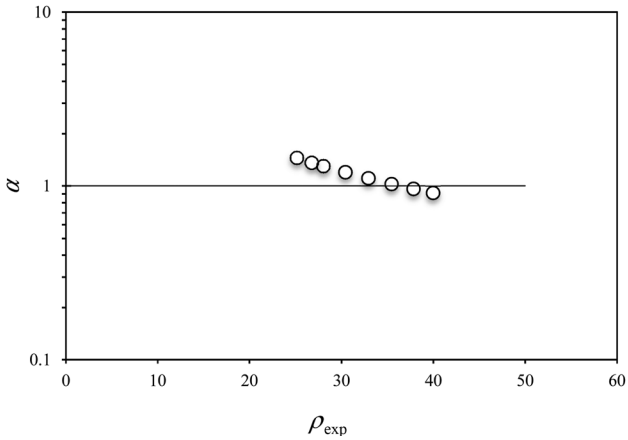

FIG. 8 Evaluation of numerical calibration factors for different types of soil for $\alpha > 1$ PV-0 is electrical resistivity of pure kaolin with PVC plate at the bottom (non-conductive boundary) and PS-0 is electrical resistivity of pure kaolin with porous stone at the bottom.

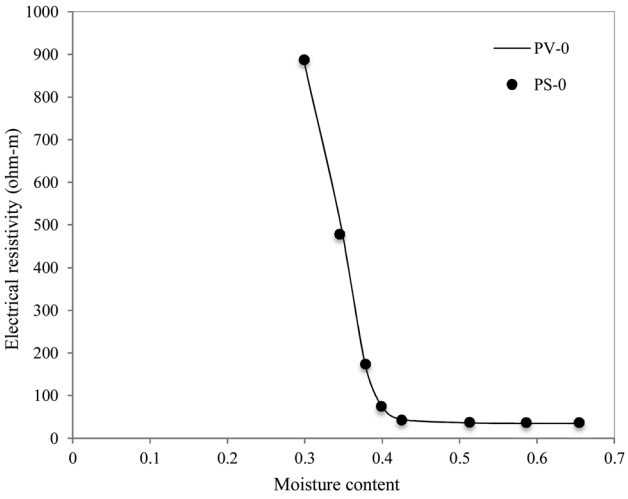

examine the changes in electrical resistivity because of changes in effective stress levels.

The changes in electrical resistivity during consolidation were evaluated in specimens of pure kaolin, M1 and M2 mixtures, as listed in the **Table 1**. In the table, LL is the liquid limit, PI is the plasticity index, G_s is the specific gravity, D_{50} is the mean grain size, and CEC is the cation exchange capacity. The electrical resistivity was measured using the previously discussed modified odometer and calibrated by the proposed calibration factors. The values obtained are plotted versus the soil's void ratio in **Fig. 9**. The results show an exponential trend consistent with the modified Archie's law, that has been developed for clays [1,30,31].

Soil electrical resistivity depends on the water content, electrical resistivity of water, and surface conductivity of bulk soil [5,12,32–35]. In this experimental program, the electrical resistivity of water was maintained constant during the consolidation tests, and as a result, the electrical resistivity deviation can be attributed to the water content and surface conductivity. As the void ratio decreases during the consolidation process, the water content drops, and, consequently, the electrical

TABLE 1 Physical properties of tested soils.

Soil Type	LL	PI	G_s	FC (%)[a]	CC (%)[b]	D_{50} (mm)	CEC (meq/100 g)
Kaolin	71	27	2.55	100	0	—	10
Mercer River sand	—	—	2.65	0	100	0.8	—
M1	—	—	2.57	90	10	—	—
M2	—	—	2.57	80	20	—	—

[a]Fines content (kaolin).
[b]Coarse content (Mercer River sand).

FIG. 9 Electrical resistivity during consolidation M1 is mixture of kaolin clay and 10 % Mercer river sand and M2 is a mixture of Kaolin clay and 20 % Mercer river sand.

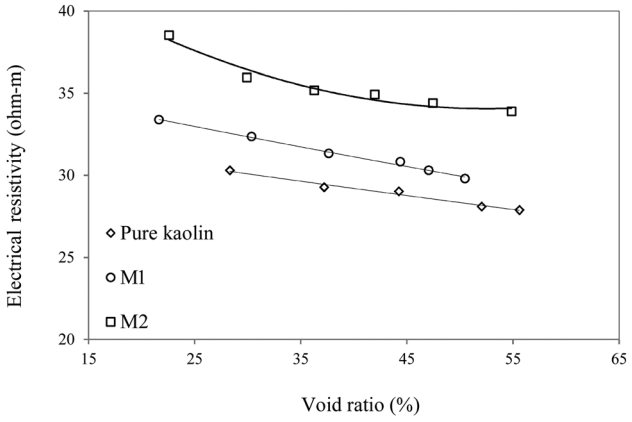

resistivity increases. For instance, a reduction of ~15 % in the porosity of kaolin clay causes ~20 % increase in electrical resistivity.

In addition, negative charges on the clay surfaces attract the cations from soil water and form a high concentration of electrically unbalanced layer of counter ions called diffuse double layer (DDL) close to the clay surfaces [32,33,36–38]. The existence of DDL layer around clay structures causes surface conduction. Adding sand to pure kaolin clay, the amount of surface charges per unit volume of soil as well as the amount of ions and volume of water in DDL layer within that specified volume will decrease. Consequently, the surface conductivity decreases and the bulk soil electrical resistivity increases, as shown in **Fig. 9** for the two mixtures.

As these experiments have been conducted in the saturated phase in the odometer cell and fully calibrated by well-verified calibration factors, the measured values for electrical resistivity can be used directly to predict the EO consolidation efficiency (Eq 1). In addition, the amount of power consumption can be accurately predicted during the electro-osmosis consolidation process to efficiently design the electro-osmosis improvement program.

Conclusions

A modified electro-odometer was developed using the configuration of the Wenner four-electrode field-testing method to measure the change in electrical resistivity of soil as the effective stress changes. A coupled numerical-experimental calibration approach was proposed in this study to account for the effect of the deviation of the proposed cell boundary conditions from the Wenner methods. Three dimensionless calibration parameters were used to describe the cell boundary conditions. Two of these parameters described the relation between the size of the specimen and the configuration of the electrodes (S/D and L/S),

whereas the third parameter expressed the relative thickness and electrical resistance of the bottom porous stone compared to the test specimen (α). For $\alpha > 1.0$, the boundary calibration factor (β) solely depends on the L/S; however, for $\alpha \leq 1$ the parameter β was influenced by the values of L/S and α. Therefore, two zones were identified to take boundary effects into the account. A calibration equation was introduced and validated for each zone. Moreover, the calibration equations were applied to the modified odometer cell, which was utilized in this study. However, for cell dimensions different from the ones used here, the proposed calibration approach in this study could be extended and used to develop suitable calibration equations.

References

[1] Archie, G. E., "The Electrical Resistivity Log as an Aid in Determining Some Reservoir Characteristics," *Trans. AIME*, Vol. 146, No. 1, 1942, pp. 54–62.

[2] Rhoades, J., Raats, P., and Prather, R., "Effects of Liquid-Phase Electrical Conductivity, Water Content and Surface Conductivity on Bulk Soil Electrical Conductivity," *Soil Sci. Soc. Am. J.*, Vol. 40, No. 5, 1976, pp. 651–655.

[3] Revil, A., Cathles, L., Losh, S., and Nunn, J., "Electrical Conductivity in Shaly Sands With Geophysical Applications," *J. Geophys. Res., Solid Earth*, Vol. 103, No. B10, 1998, pp. 23925–23936.

[4] Seladji, S., Cosenza, P., Tabbagh, A., Ranger, J., and Richard, G., "The Effect of Compaction on Soil Electrical Resistivity: A Laboratory Investigation," *Eur. J. Soil Sci.*, Vol. 61, No. 6, 2010, pp. 1043–1055.

[5] Kibria, G. and Hossain, M., "Investigation of Geotechnical Parameters Affecting Electrical Resistivity of Compacted Clays," *Geotech. Geoenviron. Eng. J.*, Vol. 138, No. 12, 2012, pp. 1520–1529.

[6] Ekwue, E. and Bartholomew, J., "Electrical Conductivity of Some Soils in Trinidad as Affected by Density, Water and Peat Content," *Biosyst. Eng.*, Vol. 108, No. 2, 2011, pp. 95–103.

[7] Mualem, Y. and Friedman, S., "Theoretical Prediction of Electrical Conductivity in Saturated and Unsaturated Soil," *Water Resour. Res.*, Vol. 27, No. 10, 1991, pp. 2771–2777.

[8] Cerato, A. B. and Lin, B., "Dielectric Measurement of Soil-Electrolyte Mixtures in a Modified Oedometer Cell Using 400 kHz to 20 MHz Electromagnetic Waves," *Geotech. Test. J.*, Vol. 35, No. 2, 2012, pp. 1–9.

[9] Fukue, M., Minato, T., Horibe, H., and Taya, N., "The Micro-Structures of Clay Given by Resistivity Measurements," *Eng. Geol.*, Vol. 54, No. 1, 1999, pp. 43–53.

[10] Kim, J. H., Yoon, H., Cho, S., Kim, Y. S., and Lee, J., "Four Electrode Resistivity Probe for Porosity Evaluation," *Geotech. Test. J.*, Vol. 34, No. 6, 2011, pp. 668–675.

[11] Kalinski, R. and Kelly, W., "Estimating Water Content of Soils from Electrical Resistivity," *Geotech Test J.*, Vol. 16, No. 3, 1993, pp. 323–329.

[12] Long, M., Donohue, S., L'Heureux, J., Solberg, I., Ronning, J. S., Limacher, R., O'Conner, P., Sauvin, G., Romoen, M., and Lecomte, I., "Relationship Between Electrical Resistivity and Basic Geotechnical Parameters for Marine Clays," *Can. Geotech. J.*, Vol. 49, No. 10, 2012, pp. 1158–1168.

[13] McCarter, W. J., "The Electrical Resistivity Characteristics of Compacted Clays," *Géotechnique*, Vol. 34, No. 2, 1984, pp. 263–267.

[14] McCarter, W. and Desmazes, P., "Soil Characterization Using Electrical Measurements," *Géotechnique*, Vol. 47, No. 1, 1997, pp. 179–183.

[15] Shang, J., "Zeta Potential and Electroosmotic Permeability of Clay Soils," *Can. Geotech. J.*, Vol. 34, No. 4, 1997, pp. 627–631.

[16] Rittirong, A., Douglas, R., Shang, J., and Lee, E., "Electrokinetic Improvement of Soft Clay Using Electrical Vertical Drains," *Geosyn. Int.*, Vol. 15, No. 5, 2008, pp. 369–381.

[17] Lefebvre, G. and Burnotte, F., "Improvements of Electroosmotic Consolidation of Soft Clays by Minimizing Power Loss at Electrodes," *Can. Geotech. J.*, Vol. 39, No. 2, 2002, pp. 399–408.

[18] Jeyakanthan, V., Gnanendran, C., and Lo, S., "Laboratory Assessment of Electroosmotic Stabilization of Soft Clay," *Can. Geotech. J.*, Vol. 48, No. 12, 2011, pp. 1788–1802.

[19] Paczkowska, B., "Electroosmotic Introduction of Methacrylate Polycations to Dehydrate Clayey Soil," *Can. Geotech. J.*, Vol. 42, No. 3, 2005, pp. 780–786.

[20] Mitchell, J. and Soga, K., *Fundamentals of Soil Behaviour*, Wiley, Hoboken, NJ, 2005.

[21] Casagrande, L., "Electroosmosis in Soils," *Géotechnique*, Vol. 1, No. 3, 1949, pp. 159–177.

[22] Wenner, F., "A Method for Measuring Earth Resistivity," *J. Franklin Inst.*, Vol. 180, No. 3, 1915, pp. 373–375.

[23] ASTM G57-06, *Standard Method for Field Measurement of Soil Resistivity Using the Wenner Four-Electrode Method*, ASTM International, West Conshohocken, PA, 1995, www.astm.org

[24] ASTM D6431-99, *Standard Guide for Using the Direct Current Resistivity Method for Subsurface Investigation*, ASTM International, West Conshohocken, PA, 1999, www.astm.org

[25] Gupta, S. and Hanks, R., "Influence of Water Content on Electrical Conductivity of the Soil," *Soil Sci. Soc. Am. J.*, Vol. 36, No. 6, 1972, pp. 855–857.

[26] Kalinski, R. and Kelly, W., "Electrical Resistivity Measurements for Evaluating Compacted-Soil Liners," *Geotech. Eng. J.*, Vol. 120, No. 2, 1994, pp. 451–457.

[27] Choo, H., Yeboah, N., and Burns, S., "Impact of Unburned Carbon Particles on the Electrical Conductivity of Fly Ash Slurry," *Geotech. Geoenviron. Eng. J.*, Vol. 140, No. 9, 2014.

[28] Lin, B. and Cerato, A. B., "Electromagnetic Properties of Natural Expansive Soils Under One-Dimensional Deformation," *Acta Geotech.*, Vol. 8, No. 4, 2013, pp. 381–393.

[29] Rinaldi, V. A. and Cuestas, G. A., "Ohmic Conductivity of a Compacted Silty Clay," *Geotech. Geoenviron. Eng. J.*, Vol. 128, No. 10, 2002, pp. 824–835.

[30] Atkins, J. E. and Smith, G., "The Significance of Particle Shape in Formation Resistivity Factor-Porosity Relationships," *Pet. Technol. J.*, Vol. 13, No. 3, 1961, pp. 285–291.

[31] Salem, H. S. and Chilingarian, G. V., "The Cementation Factor of Archie's Equation for Shaly Sandstone Reservoirs," *Pet. S. Eng. J.*, Vol. 23, No. 2, 1999, pp. 83–93.

[32] Bolt, G. H., *Soil Chemistry B: Physico-Chemical Models*, Elsevier, Amsterdam, 1979.
[33] Mojid, M., Rose, D., and Wyseure, G., "A Model Incorporating the Diffuse Double Layer to Predict the Electrical Conductivity of Bulk Soil," *Eur. J. Soil Sci.*, Vol. 58, No. 3, 2007, pp. 560–572.
[34] Olesen, T., Moldrup, P., and Gamst, J., "Solute Diffusion and Adsorption in Six Soils Along a Soil Texture Gradient," *Soil Sci. Soc. Am. J.*, Vol. 63, No. 3, 1999, pp. 519–524.
[35] Rhoades, J., Manteghi, N., Shouse, P., and Alves, W., "Soil Electrical Conductivity and Soil Salinity: New Formulations and Calibrations," *Soil Sci. Soc. Am. J.*, Vol. 53, No. 2, 1989, pp. 433–439.
[36] Bergaya, F. and Lagaly, G., *Handbook of Clay Science*, Elsevier, Amsterdam, 2013.
[37] Sheriff, R. E., *Encyclopedic Dictionary of Applied Geophysics*, Society of Exploration Geophysicists, Tulsa, OK, 2002.
[38] Mojid, M. and Cho, H., "Estimating the Fully Developed Diffuse Double Layer Thickness From the Bulk Electrical Conductivity in Clay," *Appl. Clay. Sci.*, Vol. 33, No. 3, 2006, pp. 278–286.